Research Article

Xinrui Cao* and Stefan Sinzinger

Effects of illumination on image reconstruction via Fourier ptychography

https://doi.org/10.1515/aot-2017-0048
Received July 26, 2017; accepted August 17, 2017; previously published online September 11, 2017

Abstract: The Fourier ptychographic microscopy (FPM) technique provides high-resolution images by combining a traditional imaging system, e.g. a microscope or a 4f-imaging system, with a multiplexing illumination system, e.g. an LED array and numerical image processing for enhanced image reconstruction. In order to numerically combine images that are captured under varying illumination angles, an iterative phase-retrieval algorithm is often applied. However, in practice, the performance of the FPM algorithm degrades due to the imperfections of the optical system, the image noise caused by the camera, etc. To eliminate the influence of the aberrations of the imaging system, an embedded pupil function recovery (EPRY)-FPM algorithm has been proposed [Opt. Express 22, 4960–4972 (2014)]. In this paper, we study how the performance of FPM and EPRY-FPM algorithms are affected by imperfections of the illumination system using both numerical simulations and experiments. The investigated imperfections include varying and non-uniform intensities, and wavefront aberrations. Our study shows that the aberrations of the illumination system significantly affect the performance of both FPM and EPRY-FPM algorithms. Hence, in practice, aberrations in the illumination system gain significant influence on the resulting image quality.

Keywords: Fourier ptychography; illumination design; image reconstruction.

OCIS Codes: (110.2945) illumination design; (070.0070) Fourier optics and signal processing.

***Corresponding author: Xinrui Cao,** Fachgebiet Technische Optik, Institut für Mikro- und Nanotechnologien (IMN) MacroNano®, Technische Universität Ilmenau, Postfach 100565, 98684 Ilmenau, Germany, e-mail: xinrui.cao@tu-ilmenau.de
Stefan Sinzinger: Fachgebiet Technische Optik, Institut für Mikro- und Nanotechnologien (IMN) MacroNano®, Technische Universität Ilmenau, Postfach 100565, 98684 Ilmenau, Germany

1 Introduction

The Fourier ptychographic microscopy (FPM) algorithm recovers a high-resolution complex sample image by stitching together the Fourier spectra of a variety of recorded low-resolution images. The complete Fourier spectrum can be calculated by applying the phase-retrieval concept developed in Refs. [1, 2]. However, in practice, the quality of the reconstructed image is influenced by the imperfections of the optical system, i.e. non-identical and non-uniform intensities of the illumination systems, optical aberrations of the illumination and imaging systems, image noise, and detector misalignment.

Several phase-retrieval algorithms have been proposed to improve the quality of a reconstructed image by taking into account the optical aberrations of the imaging system [3–8]. The algorithms in Refs. [6, 8] improve the quality of the object estimates as well as the initial estimate of the illumination without requiring an accurate model of the illumination wavefront. This is only valid if the illumination wavefront remains constant for all illumination angles. The algorithms in Refs. [3, 7] have been developed to recover the pupil function of the imaging system as well as the complex Fourier or Fresnel transform of the sample, simultaneously. Here, an ideal illumination system using an array of LEDs is considered. The sequentially illuminating waves are assumed to be homogeneous plane waves carrying identical intensities for all illumination angles.

In practice, the light beams of the illumination system from different angles have different intensities and are generally not uniform. Moreover, the light beams are usually not ideal plane waves. Deviations from the plane wavefront can be described as wavefront aberrations, e.g. by using Zernike polynomials [9]. Therefore, it is worth while investigating the influence of these imperfections on the quality of the reconstructed image. In particular, in this paper, we consider non-identical and non-uniform illumination intensities as well as the wavefront aberrations and discuss their influence on the reconstructed intensity image when the FPM or the embedded pupil function recovery (EPRY)-FPM algorithm is used. Our study shows that the imperfections of the illumination

system can significantly affect the performance of the FPM and the EPRY-FPM algorithm. These imperfections should be taken into account by developing robust FPM algorithms.

The paper is organized as follows. In Section 2, we introduce our illumination concept. In Section 3, we study the influence of different kinds of imperfections of the illumination system separately and compare them with the ideal case. Both the FPM and the EPRY-FPM algorithm are used. In Section 4, we set up three experiments and compare the quality of the reconstructed images after using the FPM algorithm with low-resolution intensity images obtained from the experiments. A conclusion is drawn in Section 5.

2 Illumination concept

To understand the concept of Fourier ptychography, we consider a typical illumination design in Fourier optics, which is shown in Figure 1 [10]. The compact illumination system consists of multiple individual illumination modules, which lead to different inclination angles of the illumination in the object plane and, thus, spatial shifts of the Fourier spectrum in the Fourier plane. Each illumination module consists of an LED, a spatial filter, as well as a collimator. The LEDs have the same luminous flux, the same spectrum, and can be turned on or off individually. The spatial filter in front of each LED guarantees the spatial coherence. The collimator in each module should ensure a good quality of the illumination wave in the object sample, i.e. uniform intensities as well as small wavefront aberrations.

The ideal illumination with plane waves in the object plane, the illumination aberrations, and the sample object are denoted by U_{illu}, ΔU_{illu} and U_{Obj}, respectively. The product of $(U_{\mathrm{illu}}+\Delta U_{\mathrm{illu}})$ and U_{Obj} is denoted by U_{o}, which is imaged by a 4f-imaging system. The complex amplitude of the pupil function of the imaging system is described

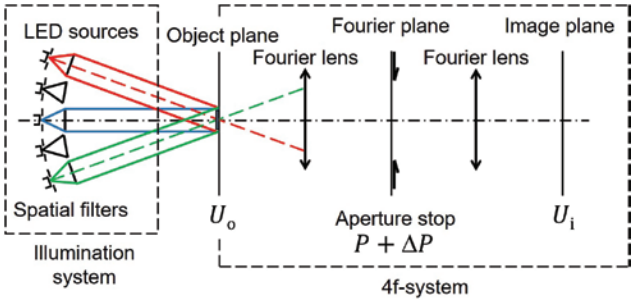

Figure 1: Illumination concept [10].

as P. By considering the aberrations of the imaging system ΔP, the corresponding amplitude transfer function of the coherent imaging system can be described as $(P+\Delta P)$. By following Ref. [11], the equivalent frequency domain representation of the complete coherent imaging system is derived as:

$$\mathcal{F}\{U_{\mathrm{i}}\}=\mathcal{F}\{(U_{\mathrm{illu}}+\Delta U_{\mathrm{illu}})\cdot U_{\mathrm{Obj}}\}\cdot(P+\Delta P) \tag{1}$$

Equation (1) shows that the complex amplitude of the image is influenced by the sample object and the illumination wave as well as the amplitude transfer function or rather the pupil function of the imaging system.

If the optical system is aberration free, and there is neither image noise nor misalignment, then, a high-resolution intensity image can be obtained from a number of low-resolution intensity images after using the FPM algorithm. If the optical system has only optical aberrations caused by the imaging system, then, these imperfections can be modeled by a common aberrated pupil function, which may be solved using the EPRY-FPM algorithm [3]. However, in practice, each illumination module may also introduce imperfections, which lead to different aberrated pupil functions for different illumination angles. In the remainder of the paper, we consider imperfect illumination systems and investigate how imperfections of the illumination system affect the quality of the reconstructed image using FPM and EPRY-FPM algorithms.

The FPM algorithm [2] comprises an iterative phase-retrieval process and a stitching process. In the stitching process of each iteration, the amplitudes in all subregions of the Fourier spectrum of the input image are replaced by the squared roots of the corresponding measured intensities, which are captured under different illumination angles. As the measured intensity images under varying illumination angles correspond to different subregions of the object spectrum, we obtain a broader spectrum than that of each subregion, which is limited by the finite aperture in the Fourier plane. At the end of each iteration, a high-resolution output image (compared to the input image) results from the Fourier transform of the broad spectrum after the stitching process. The output image is used as the input image of the next iteration. Note that the phase retrieval is achieved using overlapping subregions and keeping the phase information in each subregion unchanged during the stitching process. After a sufficient number of iterations, the iterative phase-retrieval process will converge to a stable solution [1]. Compared to the FPM algorithm, the aberrated pupil function of the imaging system is taken into account in the stitching process of the EPRY-FPM algorithm [3]. To this end, the new spectrum in each subregion consists of the current Fourier spectrum

and a weighted correction term, which uses the corresponding measured intensity image.

3 Simulation

In our numerical simulations, a picture of a spoke target is used, which has 16 bars over 360° as the sample object. A spoke target is useful for determining the resolution of the optical image because of its different spatial frequencies of the adjacent bars at different radii. We consider an illumination system consisting of nine individual illumination modules. Each kind of the imperfection, i.e. non-identical intensities for different illumination angles, non-uniform intensities of the illuminating waves, and optical aberrations of the individual illumination systems, will be studied. In each case, only one kind of the imperfections is present, and a new intensity image will be reconstructed using the FPM algorithm or the EPRY-FPM algorithm after one iteration and 100 iterations, respectively. The reconstructed intensity images obtained by assuming an aberration-free optical system after one iteration and 100 iterations are used as benchmarks.

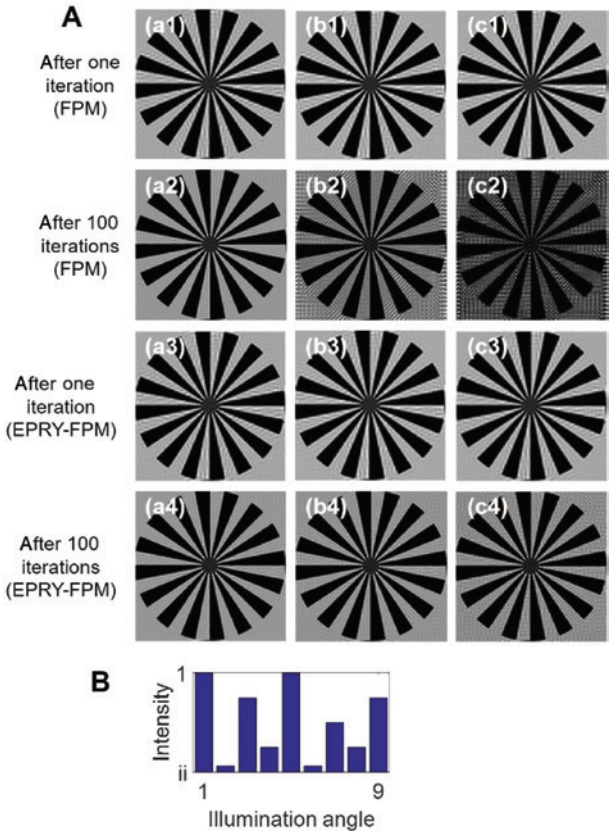

Figure 2: Influence of fluctuations of the illumination intensities. (A) (a1–a4) Reconstructed images after one iteration and 100 iterations with illumination intensity 1 using FPM and EPRY-FPM algorithms. (b1–b4) Reconstructed images after one iteration and 100 iterations with random illumination intensities in a range between 0.8 and 1. The value of ii in (B) is 0.8. (c1–c4) Reconstructed images after one iteration and 100 iterations with random illumination intensities in a range between 0.6 and 1. The value of ii in (B) is 0.6. (B) Illumination intensities for nine different illumination angles are in a range between ii and 1.

3.1 Influence of the illumination intensities

Two situations are considered. In the first situation, the intensity distribution of each illumination module is uniform, but may vary from module to module. In the second situation, the intensities of each illumination module are identical but not uniform, i.e. a Gaussian distribution is assumed.

3.1.1 Fluctuation of the illumination intensities

The simulation results shown in Figure 2 demonstrate the dependence of the FPM and EPRY-FPM algorithms on the intensities of the individual illumination systems. The results in (a1–a4) correspond to the ideal situation of identical intensities. For the results in (b1–b4), we vary the intensities in each illumination channel randomly in a range from 0.8 to 1. In (c1–c4) we vary the intensities between 0.6 and 1. After one iteration, the results with random intensities are almost the same as the result with identical intensities using the FPM and EPRY-FPM algorithms. After 100 iterations, the FPM algorithm seems to be quite sensitive to intensity fluctuations, which results in a low contrast in the reconstructed image. This means that the iteration process of the FPM algorithm is more sensitive to intensity fluctuations, and the EPRY-FPM algorithm can be used in dealing with the problems caused by the non-identical intensities from different illumination angles.

3.1.2 Uniformity of the illumination intensities

We now assume that the illumination beams at the sample object plane have a Gaussian intensity distribution as described by equation (2).

$$U_{\text{illu}}(x,y) = e^{-\frac{x^2+y^2}{2\sigma^2}} \tag{2}$$

The maximal intensity of the illumination is located at the center of the spoke target. By changing the variance σ^2, we can control the slope of the illumination intensities. In

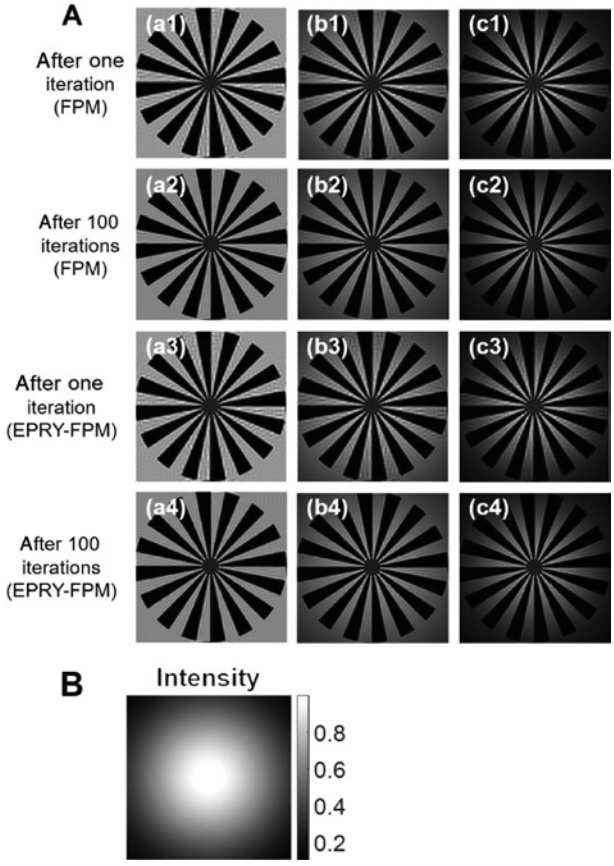

Figure 3: Influence of the uniformity of the illumination intensities. (A) (a1–a4) Reconstructed images after one iteration and 100 iterations with uniform illumination intensity using FPM and EPRY-FPM algorithms. (b1–b4) Reconstructed images after one iteration and 100 iterations with non-uniform intensity distribution shown in (B). The Gaussian beam width is $\sigma^2 = 1$. (c1–c4) Reconstructed images after one iteration and 100 iterations with non-uniform intensity distribution shown in (B). The Gaussian beam width is $\sigma^2 = 0.4$. (B) Gaussian distribution of the illumination intensity.

(b1–b4) of Figure 3, we set $\sigma^2 = 1$. In (c1–c4) $\sigma^2 = 0.4$. After one iteration and 100 iterations, the results achieved with a smaller width of the Gaussian intensity distribution using either the FPM or the EPRY-FPM algorithm exhibit a low contrast. This means that both algorithms are quite sensitive to the non-uniformity of the illumination intensities. It is also possible to individually perform the FPM algorithm on different sections of the image field. In this case, the non-uniformity of the illumination beam can be reduced.

3.2 Illumination wavefronts

We now investigate the influence of wavefront aberrations in the illuminating beams on the result of the FPM and EPRY-FPM algorithms. We assume that the intensities for various illumination angles are identical and uniform. The Zernike polynomials are used to model the wavefront aberrations of the illumination system. Here, we investigate two kinds of wavefront aberrations, i.e. astigmatism and spherical aberrations. The astigmatism and spherical aberrations are set for nine fixed illumination angles, and their peak to valley distances are varied, which are shown in Figure 4B.

The influences of astigmatism and spherical aberrations on the quality of the reconstructed intensity images are shown in Figures 4 and 5, respectively. The results with a wider range of wavefront aberrations are worse. The reconstructed intensity images after using the EPRY-FPM algorithm are not better than using the FPM algorithm. A possible reason is that, in the EPRY-FPM algorithm, the optical aberrations of the imaging system are modeled by

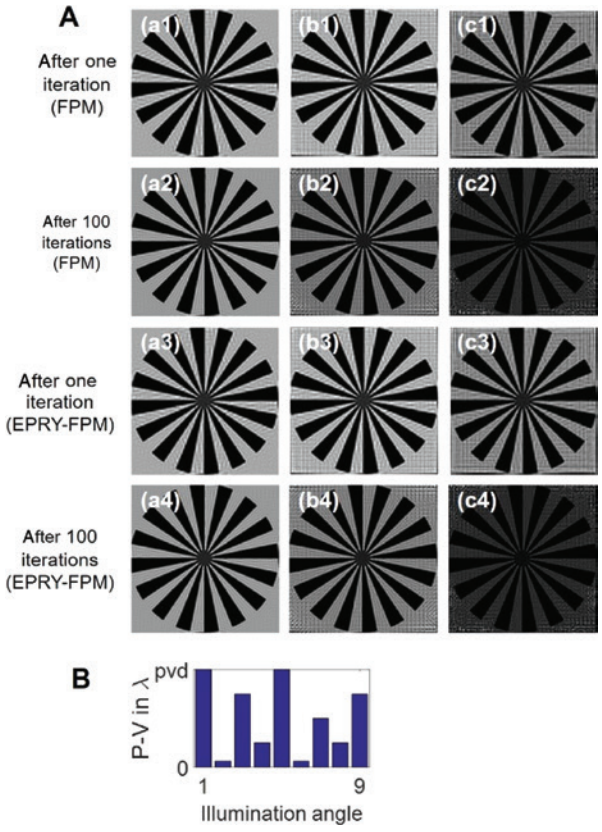

Figure 4: Influence of the astigmatism aberrations. (A) (a1–a4) Reconstructed images after one iteration and 100 iterations with no wavefront aberrations using FPM and EPRY-FPM algorithms. (b1–b4) Reconstructed images after one iteration and 100 iterations with astigmatism in the illumination system. The maximal peak to valley distance due to the aberration in (B) is pvd = 0.35 λ. (c1–c4) Reconstructed images after one iteration and 100 iterations with bigger astigmatism from the illumination system. The maximal peak to valley distance in (B) is pvd = 1 λ. (B) Peak to valley distance of the astigmatism aberrations on nine fixed illumination angles.

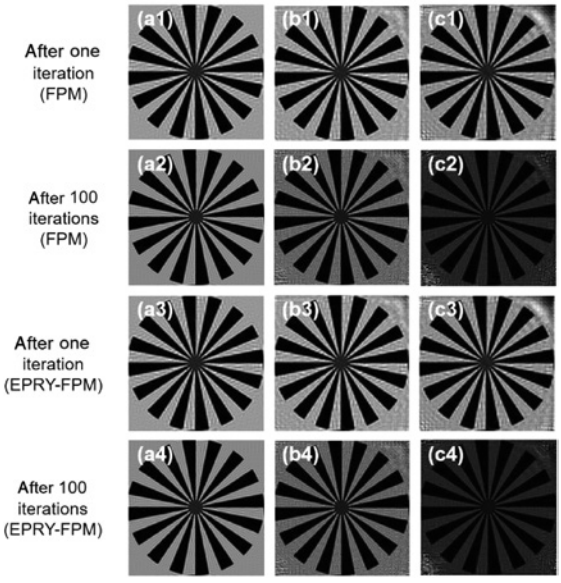

Figure 5: Influence of the spherical aberrations. (a1–a4) Reconstructed images after one iteration and 100 iterations with no wavefront aberrations using FPM and EPRY-FPM algorithms. (b1–b4) Reconstructed images after one iteration and 100 iterations with spherical aberrations from the illumination system. The maximal peak to valley distance is pvd = 3.5 λ. (c1–c4) Reconstructed images after one iteration and 100 iterations with bigger spherical aberrations from the illumination system. The maximal peak to valley distance is pvd = 5 λ.

a common aberrated pupil function $(P+\Delta P)$ in equation (1). However, different optical aberrations of the illumination system ΔU_{illu} lead to a varying aberrated pupil function of the whole optical system.

From the simulation results in this section, we can conclude that identical and uniform intensities of the illumination and lower aberrations of the illumination system are preferred, in order to achieve a better reconstruction. Moreover, to improve the performance of the FPM algorithm in real-world applications, not only the optical aberrations of the imaging system but also the imperfections of the illumination system should be taken into account.

4 Experimental investigation

To investigate the influence of the wavefront aberrations of the illumination system on the FPM algorithm or rather on the quality of the reconstructed intensity images in practice, we carried out three experiments, which vary only in the illumination systems. Compared to the first experiment with quasi ideal illumination, in the second experiment, we increase the astigmatism, whereas in the third experiment, the spherical aberration is increased.

It has been pointed out before that the alignment of the illumination system can be rather critical for the results of the FPM algorithm [12]. Here, we specifically focus on aberrations in the illumination. To this end, we assume perfect alignment in simulations (Section 3) as well as in experiments. Obviously, in experiments, wavefront aberrations in the illumination beam partially also contain angular misalignment. Thus, our general study also contains the effect of the angular misalignment.

4.1 Experimental setup

Figure 6 shows our experimental setup consisting of an illumination system, a 50/50 nonpolarizing beam splitter, a typical 4f-imaging system, and a Shack-Hartmann Sensor (SHSLab with SHSCam BR-110-GE, Optocraft GmbH, Erlangen, Bayern, Germany) for wavefront characterization. The illumination system in Figure 6 has light from a fiber-coupled LED (center wavelength 530 nm) (Thorlabs GmbH, Dachau/Munich, Bayern, Germany) via a 50/125 – 3.0 mm optical fiber cable (fiber core diameter 50 µm), optical lenses, and a rotation-tilt

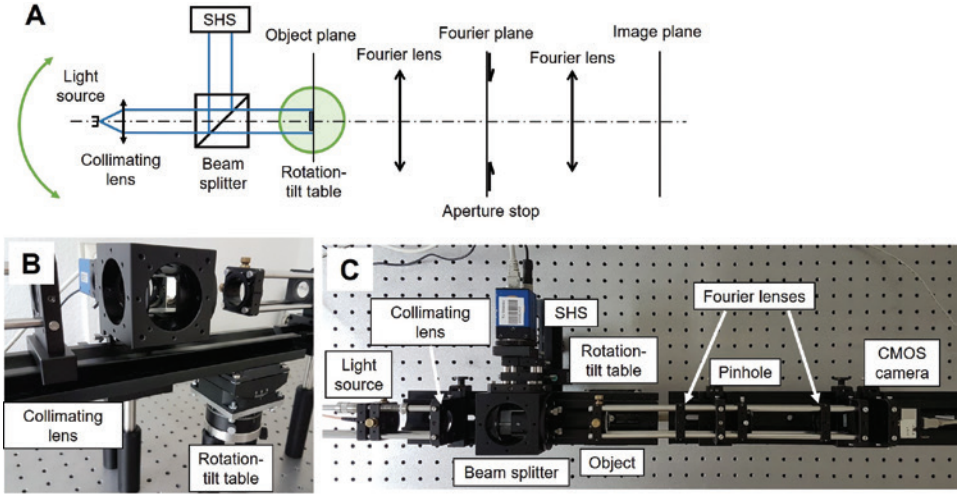

Figure 6: An illustration of the experimental setup. (A) Schematic illustration of the experimental setup. (B) Part of the illumination system with a rotation-tilt table and a collimating lens. (C) Experimental setup.

table. Note that according to Refs. [13, 14], a light source with a small diameter has a larger degree of coherence and, therefore, leads to a better reconstructed image using the FPM algorithm than the light source with a large diameter. The same conclusion is applicable to our study. The rotation-tilt table is similar to a three-dimension goniometer so that a combination of rotation angles around the vertical and horizontal axes can be realized for the experiments. The 4f-system is composed of an object, i.e. a spoke target with 36 bars over 360° adjusted in the center of the rotation-tilt table, two Fourier lenses (achromatic doublets, f = 80 mm), a pinhole with a diameter of 6.5 mm in the Fourier plane, and a CMOS camera (IDS UI-1220SE-M-GL Rev.2, IDS Imaging Development Systems GmbH, Baden-Württemberg, Germany). The beam splitter splits the light beam from the illumination system into two separate beams that are perpendicular to each other. The SHSLab can record both the wavefront and the inclination angle of the light beam, which can be used for comparing the size of the wavefront and locating the Fourier spectrum in the reconstruction process with the FPM algorithm.

The wavefront aberrations in the three experiments are influenced using different optical elements in the illumination system. In the first experiment, we use an achromatic doublet (f = 60 mm) as the collimating lens. In the second experiment, we used a cylindric lens (f = 40 mm) between the achromat and the beam splitter to generate a well-defined astigmatism. In the third experiment, we use four kinds of singlet lenses (f = 25, f = 40, f = 50 and f = 60 mm). For each illumination angle, we choose a different lens to achieve a different spherical aberration.

In each experiment, we start our measurement by recording the intensity image under the horizontal illumination angle, which is parallel to the optical axis of the imaging system. Then, by rotating the rotation-tilt table with an interval of 0.5° between every two neighboring illumination angles, we take another intensity image and so on. In the first experiment, we have taken 81 images. In the second and the third experiments, we have recorded 25 intensity images each.

4.2 Reconstructed intensity images

In the first experiment, the measured low-resolution intensity image under the horizontal illumination angle and the reconstructed intensity images with different numbers of low-resolution intensity images after using the FPM algorithm are shown in Figure 7. By increasing the number of low-resolution images (up to 25), we obtain reconstructed images with increasing resolution. If more low-resolution images are used, i.e. more than 48, the quality of the reconstructed images deteriorates, which can be caused by a relatively large image noise for large illumination angles. However, compared to the first experiment, in the second and the third experiments, we observe that the quality of the reconstructed intensity images becomes worse with 25 measured low-resolution images because of the enlarged wavefront aberrations.

To make a clear comparison between the reconstructed images from all the experiments, we show in Figures 8–10 the reconstruction results with fewer low-resolution images, which are obtained in the

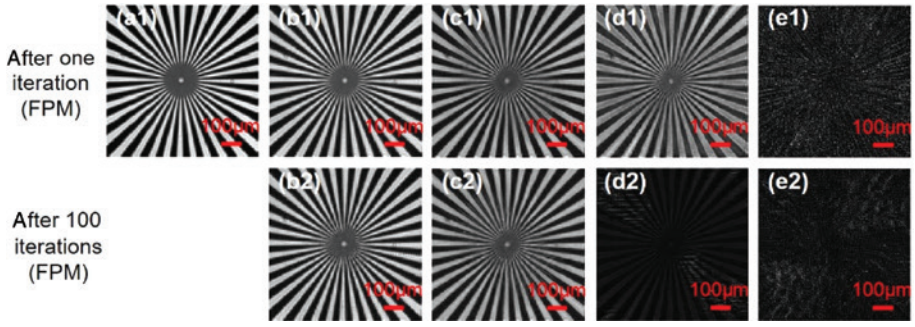

Figure 7: Reconstructed intensity images with the measured low-resolution images in the first experiment. (a1) A single intensity image taken under the horizontal illumination angle. The intensity images in (b1, b2); (c1, c2); (d1, d2); and (e1, e2) are reconstructed using the FPM algorithm with 9, 25, 48 and 81 low-resolution images, respectively.

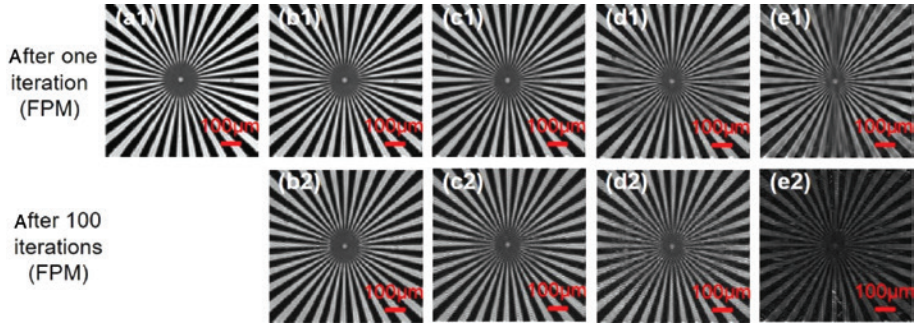

Figure 8: Reconstructed intensity images with low-resolution images taken under different vertical illumination angles in the first experiment. (a1) A single intensity image taken under the horizontal illumination angle. The intensity images in (b1, b2); (c1, c2); (d1, d2); and (e1, e2) are reconstructed using the FPM algorithm with three, five, seven and nine low-resolution images, respectively.

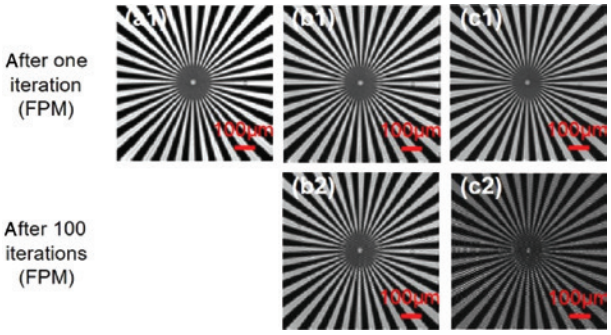

Figure 9: Reconstructed intensity images with low-resolution images taken under different vertical illumination angles in the second experiment. (a1) A single intensity image taken under the horizontal illumination angle. The images in (b1, b2) and (c1, c2) are reconstructed using the FPM algorithm with three and five low-resolution images, respectively.

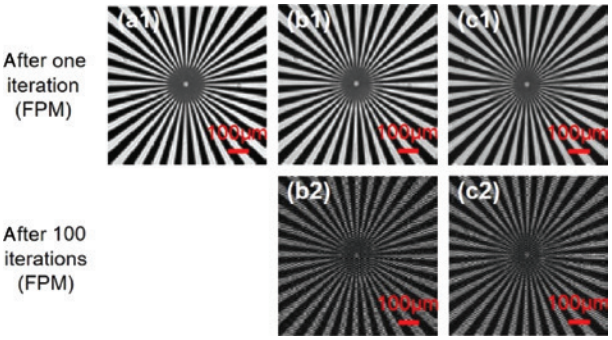

Figure 10: Reconstructed intensity images with low-resolution images taken under different vertical illumination angles in the third experiment. (a1) A single intensity image taken under the horizontal illumination angle. The images in (b1, b2) and (c1, c2) are reconstructed using the FPM algorithm with three and five low-resolution images, respectively.

first experiment, the second experiment, and the third experiment, respectively. These results correspond to the Fourier spectrum in the vertical direction in the Fourier plane. The quality of the images reconstructed with three and five low-resolution images in Figures 9 and 10 is worse than the reconstructed images with the same number of low-resolution images in Figure 8. From the experimental results in this section, we can conclude that, if the FPM algorithm is used, the quality of the image reconstruction highly depends on the quality of the illumination wavefront.

5 Conclusion

In this paper, we study the influence of illumination imperfections on the quality of the reconstructed images when using the FPM or the EPRY-FPM algorithm. The simulation results show that the reconstructed images can be distorted by variation and non-uniformity of the illumination intensities as well as optical aberrations of the illumination waves. The experimental results match the simulation results. Therefore, to further improve the FPM and EPRY-FPM algorithms, the imperfections of the illumination system need to be taken into account. It is worth noting that different illumination imperfections under varying illumination angles can break the consistency between every two neighboring Fourier spectra of the sample object in their overlapping regions. In general, it is difficult to remove the illumination aberrations by extending the method in the EPRY-FPM algorithm. In the future, it will be important to study how to efficiently remove the illumination aberrations.

Acknowledgments: The authors gratefully acknowledge the support by the Deutsche Forschungsgemeinschaft (DFG) in the framework of Research Training Group "Tip- and laser-based 3D-Nanofabrication in extended macroscopic working areas" (GRK 2182) at the Technische Universität Ilmenau, Germany.

References

[1] J. R. Fienup, Appl. Opt. 21, 2758–2769 (1982).
[2] G. Zheng, R. Horstmeyer and C. Yang, Nat. Photonics 7, 739–745 (2013).
[3] X. Ou, G. Zheng and C. Yang, Opt. Express 22, 4960–4972 (2014).
[4] J. M. Rodenburg and H. M. L. Faulkner, Appl. Phys. Lett. 85, 4795–4797 (2004).
[5] H. M. L. Faulkner and J. M. Rodenburg, Ultramicroscopy 103, 153–164 (2005).
[6] M. Guizar-Sicairos and J. R. Fienup, Opt. Express 16, 7264–7278 (2008).
[7] P. C. Konda, J. M. Taylor and A. R. Harvey, Proc. SPIE 9630, 96300X (2015).
[8] A. M. Maiden and J. M. Rodenburg, Ultramicroscopy, 109, 1256–1262 (2009).
[9] J. D. Schmidt, in 'Numerical Simulation of Optical Wave Propagation with Examples in MATLAB' (Bellingham, WA: SPIE, 2010), pp. 65–68.
[10] X. Cao, M. Bichra, D. Fischer, M. Krojer, H. Prause, et al., in 'Illumination Design for Fourier Ptychography', European Optical Society Annual Meeting (EOSAM) Berlin (26.-30.09.2016).
[11] J. W. Goodman, in 'Introduction to Fourier Optics', 2nd ed. (McGraw-Hill Publishers, New York, 1996) pp. 135–136.
[12] R. Horstmeyer, X. Qu, J. Chung, G. Zheng and C. Yang, Opt. Express 22, 24062–24080 (2014).
[13] R. Horstmeyer and C. Yang, Opt. Express 22, 338–358 (2014).
[14] D. Karthaus, M. Giehl, O. Sandfuchs and S. Sinzinger, Appl. Opt. 56, 5234–5241 (2017).

Xinrui Cao
Fachgebiet Technische Optik, Institut für Mikro- und Nanotechnologien (IMN) MacroNano®, Technische Universität Ilmenau, Postfach 100565, 98684 Ilmenau, Germany
xinrui.cao@tu-ilmenau.de

Xinrui Cao was born in Shandong, China. She received her MSc degree in Mechanical Engineering from the Technische Universität Ilmenau in 2014. Since then, she is a PhD student in the Department of Optical Engineering at the Technische Universität Ilmenau. Since April 2017, she is a member of the Research Training Group on 'Tip- and laser-based 3D-Nanofabrication in extended macroscopic working areas' funded through the German Research Foundation (DFG). Her research interest is illumination design for imaging systems.

Stefan Sinzinger
Fachgebiet Technische Optik, Institut für Mikro- und Nanotechnologien (IMN) MacroNano®, Technische Universität Ilmenau, Postfach 100565, 98684 Ilmenau, Germany

Stefan Sinzinger received his Dipl.-Phys. and Dr degrees from the Friedrich-Alexander Universität Erlangen-Nürnberg, Institute for Applied Optics (Prof Dr A.W. Lohmann) in 1989 and 1993, respectively. In 2002, he became Professor for Optical Engineering ('Technische Optik') at the Technische Universität Ilmenau. Among numerous publications in international journals and conferences, Stefan Sinzinger is the co-author of the textbook 'Microoptics' and editor of the textbook 'Optical Information Processing' (author A.W. Lohmann). His current research focuses on the design, integration, fabrication, and application of (micro-) optical elements and hybrid optical (micro-) systems for innovative imaging and illumination.